Journal of Thermal Analysis, Vol. 44 (1995) 777-793

HEAT TRANSFER IN DEFORMATION CALORIMETERS

*R. E. Lyon and P. J. Raboin**

Federal Aviation Administration Technical Center, Atlantic City International Airport, NJ 08405, USA

(Received January 24, 1994; in revised form March 28, 1994)

Abstract

A simple one-dimensional, axisymmetric model of a gas-pressure deformation calorimeter containing a lumped heat source accounts for observed pressure changes in terms of conductive and radiant components of heat transfer. Agreement is generally good between experimental data and the predicted calorimeter response for the range of source dimensions, heating rates, and test temperatures investigated in the study.

Keywords: deformation calorimetry, gas-pressure calorimeter, heat transfer, thermomechanics

Introduction

A new version of a previously described [1–3] deformation calorimeter has been developed to simultaneously measure the heat and work of solid deformation. The calorimeter is a heat-flux device which senses the differential pressure change in a gas at constant differential volume surrounding a sample which is deformed along the centerline of a sealed sample chamber, as illustrated schematically in Fig. 1. The sample is deformed in tension via an Invar pullwire exiting the bottom of the sample cell through an airtight, frictionless, mercury-drop seal. An identical pullwire located in a reference cell compensates for volume-induced pressure changes in the sample cell caused by displacing the wire, so that the differential pressure is independent of the position of the pullwires, i.e., the axial strain on the sample. In the absence of sample dilatation any transient pressure change during the deformation of a solid sample is the result of a temperature rise in the gas caused by a heat flow between the sample and the cell wall. The pressure-volume effects resulting from sample dilatation can be nearly eliminated by choosing samples of sufficiently small dimensions that the fractional change in gas volume due to sample dilatation is negligible in comparison to the pressure changes associated with the thermal processes.

* University of California, Lawrence Livermore National Laboratory, Livermore, CA 94550, USA

0368–4466/95/ $ 4.00

John Wiley & Sons, Limited
Chichester

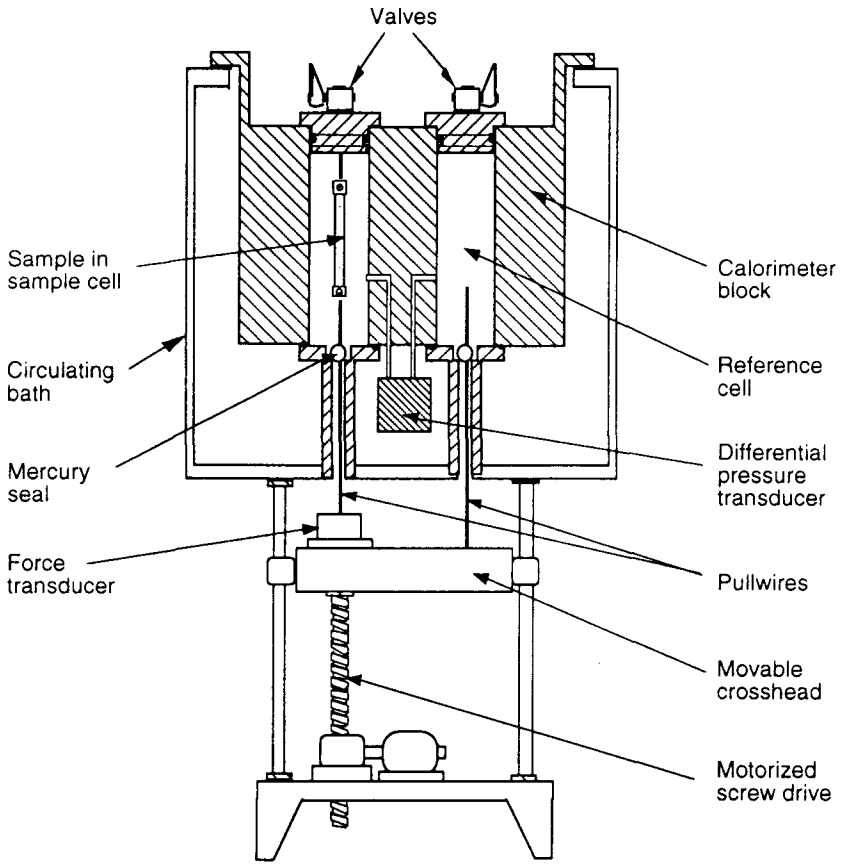

Fig. 1 Gas-pressure deformation calorimeter

In a previous paper [1] equations were derived for the steady-state and transient pressure response by assuming a calorimeter model which considers only conductive heat transfer between the heat generation source and the sample cell wall. For sample dimensions of practical interest size effects were calculated to be negligible for the conduction model. Since that time experimental data have been obtained which indicate that sample size effects are significant with regard to both the steady-state and transient pressure response of the calorimeter. The purpose of this paper is to extend the previous analyses to include radiant heat transfer and sample size effects in an attempt to quantify the heat exchange processes which occur in gas-pressure, heat-flux, microcalorimeters. A simple axisymmetric model of the calorimeter with a lumped source term is used to obtain analytic solutions which correct for sample mass and size effects on observed pressure response. Agreement between model predictions and experimental data for well defined heating histories and source properties would

confirm the proposed mechanisms of heat transfer and provide a methodology for interpreting calorimeter data from more complicated specimen geometries.

Theory

The gas-pressure calorimeter is considered to be a one-dimensional, axisymmetric system with radial heat conduction and radiation. The calorimeter ends are ignored and only the radial direction is considered. Relationships between the heat generation rate by a source, the resulting temperature distribution in the calorimeter cell, and the volumetric average pressure are required. A cylindrical heat source of radius, r_i, represents the deforming sample or resistance heating wire located along the centerline of a hollow cylindrical cell of radius, r_o, and length, L, in a calorimeter block of large thermal mass, as illustrated in Fig. 2. The annular space between the source and cell wall is occupied by a quiescent gas (usually air) at initial temperature, T_o, and pressure, P_o.

The applicable form of the lumped first law of thermodynamics for a heat source with a time-dependent, volumetric, internal heat generation rate, $\dot{Q}_i$, when no work is done is

$$\rho C V_i \frac{\partial \theta}{\partial t} = \dot{Q}_i - \dot{Q}_o \tag{1}$$

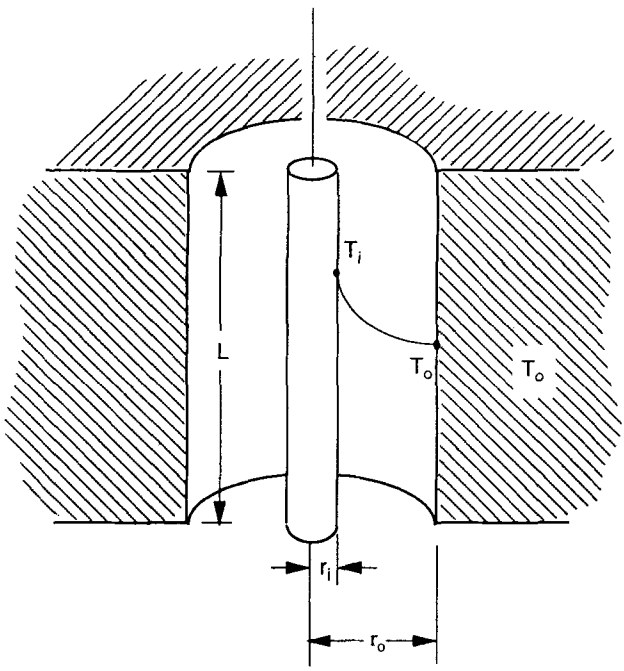

Fig. 2 Geometry of calorimeter model

The instantaneous temperature, $\theta=(T_i-T_o)$, is the temperature difference between the source at uniform temperature, T_i, and the constant cell wall temperature, T_o. The internal energy change of the heat source is represented by the left hand side of Eq. (1) where ρ is the density and, C, the heat capacity of the source having volume, V_i. The right hand side of Eq. (1) is the heat flow balance for the source expressed as the difference between the rate of heat generation into the control volume $\dot{Q}_i$, and the rate of heat transfer out of the control volume to the isothermal calorimeter block $\dot{Q}_o$. Typical temperature changes associated with microwatt-level heat flows are less than one degree i.e. $\theta \leq 1$ K, so that heat transfer from the source to the calorimeter wall through the surrounding gas is primarily by conduction and radiation. Consequently, $\dot{Q}_o = \dot{Q}_c + \dot{Q}_r$, where $\dot{Q}_c$ and $\dot{Q}_r$ are the heat transfer rates by conduction and radiation, respectively, and

$$\rho C V_i \frac{\partial \theta}{\partial t} = \dot{Q}_i - [\dot{Q}_c + \dot{Q}_r] \tag{2}$$

The instantaneous heat transfer rate by conduction through a gas of thermal conductivity, k_g, in the concentric cylindrical geometry is assumed to be

$$\dot{Q}_c = \frac{-2\pi k_g L}{\ln\left(\frac{r_i}{r_o}\right)} \theta \tag{3}$$

The net rate of radiant heat transfer between the source and cell wall is given by (4)

$$\dot{Q}_r = \frac{\sigma A_i [T_i^4 - T_o^4]}{\frac{1}{\varepsilon_i} + \frac{A_i}{A_o}\left(\frac{1}{\varepsilon_o} - 1\right)} \tag{4}$$

where, $\sigma=5.7\times10^{-8}$ w/m^2-K^4 is the Stefan-Boltzman constant and, A_i, A_o, are the surface areas of the source and calorimeter cell wall respectively with, ε_i, ε_o the associated emissivities. The fourth-power temperature difference in Eq. (4) can be expanded about a mean temperature, $\bar{T}=(T_i+T_o)/2$, with the result that; $(T_i^4-T_o^4)=4\bar{T}^3\theta+\bar{T}^3\theta^3$. For temperature differences, θ, of only a few degrees we can set, $\bar{T}\approx T_o$, and obtain, $(T_i^4-T_o^4) \approx 4T_o^3\theta$, to 99% accuracy for T_o near ambient.

For all geometries of interest, $A_i << A_o$, so that the net rate of radiant heat flow from the cylindrical source to the calorimeter cell wall from Eq. (4) becomes simply

$$\dot{Q}_r = 8\pi r_i L \sigma \varepsilon_i T_o^3 \, \theta \tag{5}$$

From Eqs (2, 3 and 5) the applicable version of the lumped energy equation for the heat source in the calorimeter becomes

$$\rho C V_i \frac{\partial \theta}{\partial t} = \dot{Q}_i - \frac{\theta}{R} \tag{6}$$

or equivalently

$$\frac{\partial \theta}{\partial t} + \frac{1}{\tau}\theta = \frac{R}{\tau}\dot{Q}_i \tag{7}$$

with

$$R = \frac{\ln (r_o/r_i)}{(2\pi k_g L) + [(8\pi r_i L \sigma \varepsilon_i T_o^3) \ln (r_o/r_i)]} \tag{8}$$

the external resistance to heat flow having units of K/Watt, and τ, the time constant of the source given by

$$\tau = \frac{\rho C r_i^2 \ln (r_o/r_i)}{2k_g + 8\pi r_i \sigma \varepsilon_i T_o^3 \ln (r_o/r_i)} \tag{9}$$

In order for a lumped analysis of the heat source in the calorimeter to be valid the resistance to heat flow within the source must be small compared to the external resistance to heat flow by the surrounding gas so that temperature gradients within the source are negligible and the source can be considered to have a single, uniform temperature, T_i. The relevant dimensionless variable in this regards is the Biot modulus, Bi, which represents the ratio of the conductive, internal resistance to heat transfer, $(V_i/A_i)/k_s$, to the external resistance to heat transfer, RA_i, for R defined by Eq. (8) and a source of thermal conductivity k_s. An error of less than five percent using a lumped formulation requires that Bi<0.1, i.e.

$$\mathrm{Bi} = \frac{(V_i/A_i)/k_s}{RA_i} \leq 0.10 \tag{10}$$

In anticipation of the calibration experiments in the following section the Biot modulus is evaluated for the maximum heating wire radius used in the studies, $r_i = 0.5$ mm, corresponding to a source volume $V_i = \pi r_i^2 L$, and surface area $A_i = 2\pi r_i L$. The calorimeter cell has a radius, $r_o = .011$ m, length,

L= 0.287 m, and contains air of thermal conductivity, k_g= .0261 W/m-K, at 298 K and atmospheric pressure. For a Nichrome heating wire thermal conductivity, k_s= 13 W/m-K, the Biot modulus is

$$\mathrm{Bi} = \frac{k_g + [4r_i\sigma\varepsilon_i T_o^3 \ln (r_o/r_i)]}{2k_s \ln (r_o/r_i)} \approx 4\times10^{-4} \tag{11}$$

well within the range of applicability for a lumped analysis of the source.

An exact solution for θ cannot be obtained from Eq. (7) without specifying a particular heating history. However the general solution for θ for the initial condition θ= 0, at t= 0, is

$$\theta(t) = R \int_0^t \frac{\exp[-(t-\xi)/\tau]}{\tau} Q_i d\xi \tag{12}$$

Next it is necessary to relate the differential gas pressure in the calorimeter to the temperature difference, $\theta(t)$. To do this assume an ideal gas at initial pressure P_o, for which the differential pressure change $\Delta P(t)$, is proportional to the instantaneous volume average temperature,

$$\Delta P(t) = \frac{P_o}{T_o} \frac{1}{V} \int_V \theta(t) dV \tag{13}$$

Substitute the temperature difference of Eq. (12) into the integrand of Eq. (13) and separate geometric and temporal quantities to obtain the following functional form the quasi-isothermal gas-pressure calorimeter response to an arbitrary heat flow to/from a source of fixed dimensions

$$\Delta P(t) = \left[\frac{P_o}{T_o} \frac{1}{V} \int_V R dV\right]\left[\int_0^t \frac{\exp[-(t-\xi)/\tau]}{\tau} Q_i d\xi\right] =$$

$$= [G(x)][F(t,\dot{Q})] \tag{14}$$

Evaluating the first bracketed term on the right hand side of Eq. (14) requires an integration over the gas volume, $V= \pi(r_o^2-r_i^2)L$, with $dV= -2\pi L r_i dr_i$. Defining a new dimensionless variable, $x= r/r_o$, and substituting Eq. (8) into the integrand for R, with the condition that, $r_i << r_o$. The bracketed term $G(x)$, is expressed as

$$G(x) \equiv \left[\frac{P_o}{T_o} \frac{1}{V} \int_v R dV\right] = \frac{P_o}{4\pi k_g L T_o} \int_x^{i^1} \frac{-x\ln(x^4)}{1-\beta\ln(x)} dx \tag{15}$$

where $\beta = 4r_i\varepsilon_i\sigma T_o^3/k_g$ is a dimensionless ratio of radiation/conduction terms which is a constant for a particular source volume. The term, $P_o/4\pi k_g L T_o \equiv G(0)$ is the calorimeter response for a line source, $x = 0$. The integral term on the right hand side of Eq. (15) approaches unity as, x, approaches zero, i.e. $G(x) \rightarrow G(0)$, as $x \rightarrow 0$. $G(x)$ is a time-independent function of the source, cell, and gas properties and geometries at fixed temperature which cannot be solved analytically but is easily evaluated by numerical integration between the indicated limits: $x_i = r_i/r_o$ and $x_i = r_o/r_o = 1$.

The last bracketed term on the right hand side of Eq. (14)

$$F(t,\dot{Q}) = \int_0^t \frac{\exp[-(t-\xi)/\tau]}{\tau} Q_i d\xi$$

is a convolution integral of the arbitrary heating history, Q_i, with the single-exponential kernel function, $(1/\tau)\exp(-t/\tau)$, and is a function of time only for fixed test geometry and temperature (5). In order to test the axisymmetric model of the calorimeter containing a lumped heat source experimentally Eq. (14) was solved by substituting the simple square-wave heating history,

$$Q_i = [U(t) - U(t-t')]\dot{Q}_i^o \tag{16}$$

with the result

$$\Delta P(t) = G(x)\dot{Q}_i^o(1 - \exp[-t/\tau]) \qquad (t < t') \tag{17a}$$

$$\Delta P(t) = G(x)\dot{Q}_i^o(\exp[-t/\tau]) \qquad (t \geq t') \tag{17b}$$

The steady-state pressure response of the calorimeter, $\Delta P(\infty)$, to a constant rate of heat generation by the source, $\dot{Q}_i^o$, is obtained analytically by setting $t = \infty$, in Eq. (17a)

$$\Delta P(\infty) = G(x)\dot{Q}_i^o \tag{18}$$

which corresponds to an experimental observation when $t' >> \tau$. Figure 3 shows the heating history of Eq. (16) and the predicted pressure response of the calorimeter according to Eq. (17) for a heating duration, $t' >> \tau$.

In the following sections the validity of the axisymmetric, one-dimensional calorimeter model is tested by comparing experimental and predicted values of τ and $G(x)$ for different source dimensions and test temperatures. Equation (18) provides a simple experimental procedure for determining $G(x)$ using steady-state gas pressure measurements at constant heat flow for various source diame-

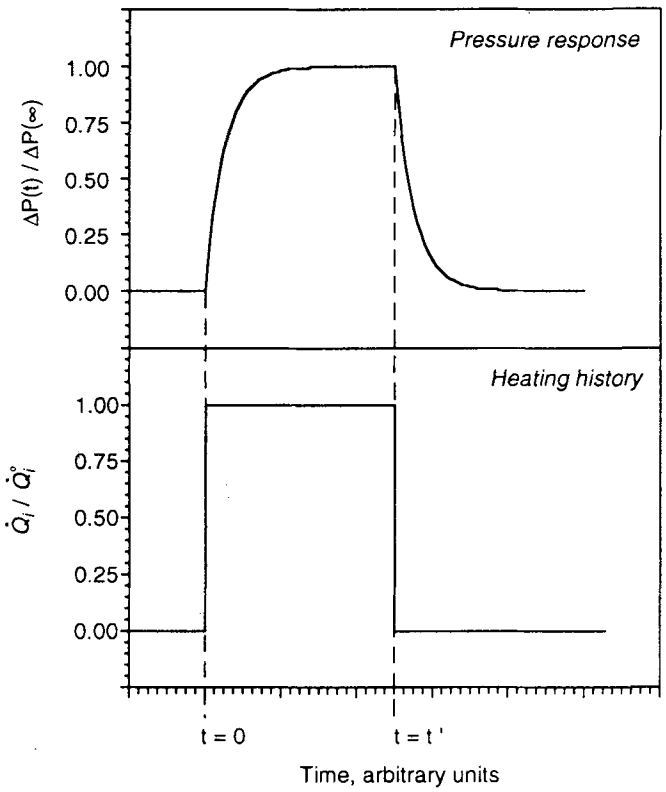

Fig. 3 Predicted pressure response to square wave heating history for $t' >> \tau$

ters, temperatures, and gas properties for comparison to values predicted by Eq. (15). Equation (17) allows for the determination of τ as a function of source and gas properties and geometry from the transient response to a step change in heat flow for comparison to Eq. (9)

Experimental

Electrical resistance heating experiments were performed in the calorimeter using 15 cm long Nichrome V wires (Stableohm 650, California Fine Wire) of diameter 0.102, 0.203, 0.320, 0.406, 0.635, 0.813 and 1.016 mm. A source length effect study was conducted using 5, 10 and 15 cm lengths of the .320 mm wire. The heating wires were attached via gold pin connectors to Teflon clad, 24G copper wire which exited the top and bottom of the calorimeter cell through air-tight seals. The electrical resistance of the Nichrome heating wires was determined to an accuracy of ±1 mohm using a 4-arm bridge (Hewlett-Packard Model 3455A). A programmable current source (Keithley

Model 220) provided a square wave current pulse of adjustable duration and amplitude to the heating wires. The current in the Nichrome resistance wire contained in the calorimeter cell was monitored to ±0.1 mA using a multimeter (Fluke Model 77) in parallel with the current source and Nichrome heating wire. The rate of heat generation by the wire in the calorimeter cell was calculated form the measured current, I, and wire resistance, Ω as, $\dot{Q}_i^\circ = I^2\Omega$. The electrical heating experiments were conducted at calorimeter cell temperatures of 278, 298, 318 and 338 K.

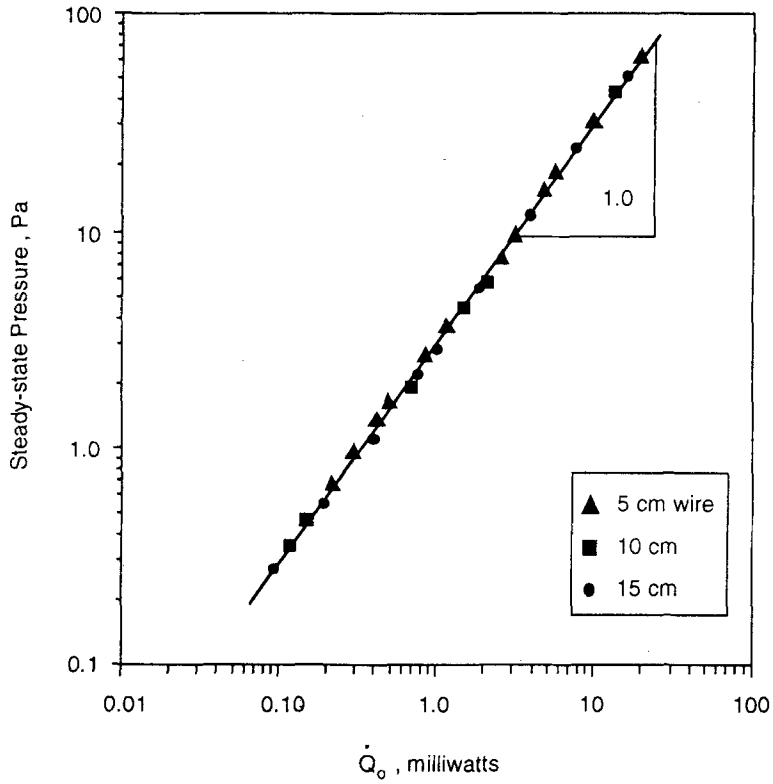

Fig. 4 Steady-state pressure *vs.* heating rate for 5, 10 and 15 cm long heating wires

The transient and steady-state gas pressure change in the calorimeter cell was measured for several heating rates between 0.10 and 100 mW. A linear regression of these data, weighted for low heating rates and forced through the origin, was performed to determine the ratio of steady-state pressure to constant heating rate, $\Delta P(\infty)/\dot{Q}_i^\circ$, for each individual wire diameter at a particular cell temperature. The average time constant, τ, for the pressure response was determined in accordance with Eq. (17) as the time required for the pressure to rise to 63% of the steady-state value after initiation of current flow, or fall to 37%

of the steady-state value after the cessation of heating. The transient pressure response closely approximated single exponential behavior in all cases. The numerical value of τ obtained from the rise and fall time were in exact agreement.

Results

The measured ratio of the steady-state pressure for a constant heat flow, $\Delta P(\infty)/\dot{Q}_i^o$, and the experimental values of the time constant, τ, are reported in Tables 1 and 2, respectively, for the combinations of wire diameter and temperature examined in the study. A small but systematic decrease in $\Delta P(\infty)/\dot{Q}_i^o$, with increasing wire (source) diameter is observed for each individual cell temperature. A more pronounced decrease in $\Delta P(\infty)/\dot{Q}_i^o$ with temperature at constant source diameter is also observed.

Table 1 Experimental values of steady-state pressure response per unit heat flow, $\Delta P(\infty)/\dot{Q}_i^o$ (KPa /Watt), for different heating wire diameters and cell temperatures

Heating wire diameter/ mm	Steady-state pressure/heat flow, $\Delta P(\infty)/\dot{Q}_i^o$/ KPa·Watt^{-1}			
	T_0 = 278 K	T_0 = 298 K	T_0 = 318 K	T_0 = 338 K
0.102	–	3.53	–	–
0.203	4.00	3.50	3.09	2.76
0.320	–	3.45	–	–
0.406	4.03	3.42	2.92	2.59
0.635	–	3.31	–	–
0.813	3.78	3.20	2.81	2.43
1.016	–	3.14	–	–

Table 2 Experimental values of time constant, τ (seconds), for different heating wire diameters and cell temperatures

Heating wire diameter/ mm	Time constant, τ/ sec			
	T_0 = 278 K	T_0 = 298 K	T_0 = 318 K	T_0 = 338 K
0.102	–	1.9	–	–
0.203	4.5	4.5	4.2	4.0
0.320	–	9.0	–	–
0.406	12.8	12.0	11.5	11.2
0.635	–	26.5	–	–
0.813	37.5	36.5	33.0	31.0
1.016	–	52.0	–	–

Representative data for steady-state pressure, $\Delta P(\infty)$, *vs.* heating rate, $\dot{Q}_i^o$, obtained at 298 K for 5, 10 and 15 cm lengths of the .203 mm diameter wires are shown in Fig. 4. A linear relationship between steady-state pressure and heating rate, independent of source length over the range investigated, is deduced from the unit slope on the log-log plot, as predicted by Eq. (18). Linear regression of the data in Fig. 4 replotted in linear coordinates gives the value, $\Delta P(\infty)/\dot{Q}_i^o = 3.50$ KPa/W which is reported in Table 1 for this temperature and wire diameter.

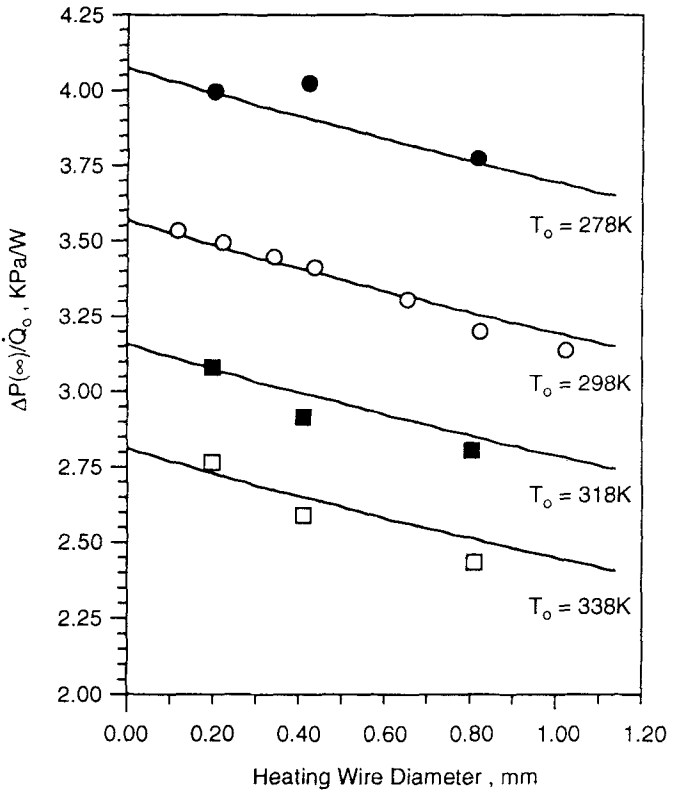

Fig. 5 $G(x)$ (—) as a function of heating wire diameter compared to measured $\Delta P(\infty)/\dot{Q}_i^o$ values at cell temperature of 278(•), 298(o), 318(■) and 338 K (□)

Figure 5 compares all of the experimental data in Table 1 for $\Delta P(\infty)/\dot{Q}_i^o$ at different source dimensions and cell temperatures to the predicted values $\Delta P(\infty)/\dot{Q}_i^o = G(x)$, calculated using Eq. (15). Tabulated values for the thermal conductivity of air (6) were interpolated to give, $k_g = .0245$, .0261, .0276, and .0292 W/m-K, at cell temperatures, $T_o = 278$, 298, 318, and 338 K, respectively. The calorimeter cell length, $L = 0.287$ m, and an assumed emissivity of, $\varepsilon = 1.0$, for the Nichrome wires were also used in Eq. (15) to calculate $G(x)$. It

is observed that the calculated values for $G(x)$ *vs.* wire diameter at each temperature are in essentially quantitative agreement with the experimental $\Delta P(\infty)/Q_i^\circ$ data.

To simplify the evaluation of $G(x)$ an empirical equation was obtained by curve-fitting the numerical results for the integral Eq. (15) plotted in Fig. 5. The resulting analytical approximation of Eq. (15) for use with air as the heat transfer medium in the calorimeter and sample emissivities of unity is

$$G(x) = G(0)\left[1 - \frac{5}{2}\left(\frac{T_o}{T_{ref}}\right)^2 x + \frac{14}{3}\left(\frac{T_o}{T_{ref}}\right)^2 x^2\right] \tag{19}$$

where, T_{ref}= 298 K, is a reference temperature and as previously, $x= r_i/r_o$, and $G(0)= P_o/4\pi k_g L T_o$. Equation 19 is within 1% of the exact results for $G(x)$ plotted in Fig. 5, and allows direct evaluation of $G(x)$ without numerical integration via Eq. (15) for each choice of sample dimension and test temperature.

The effect of sample thickness changes on the value of $G(x)$ during uniaxial deformation in the calorimeter is readily calculated from Eq. (19) by assuming

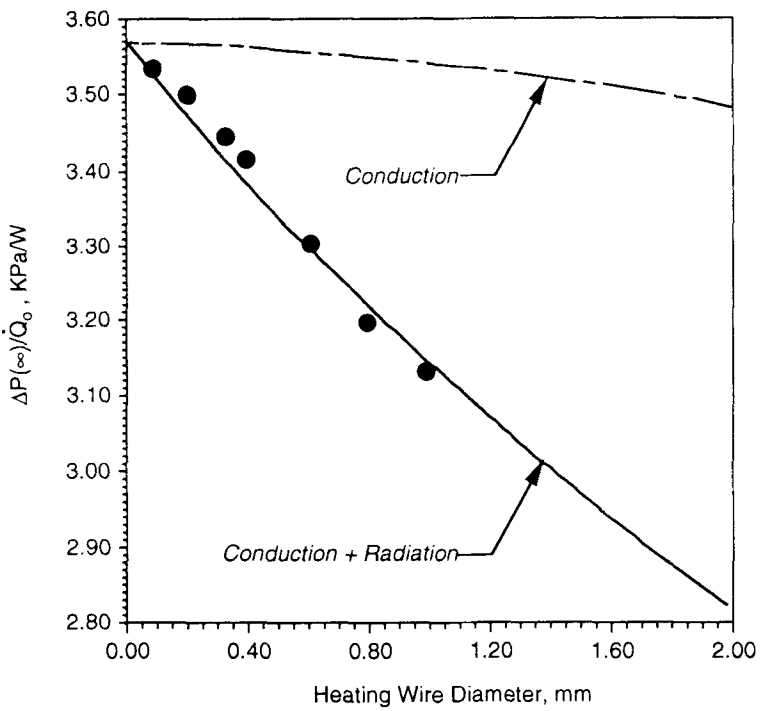

Fig. 6 $G(x)$ as a function of heating wire diameter for heat transfer by conduction (---) and by combined conduction and radiation (—) compared to measured $\Delta P(\infty)/Q_i^\circ$ values (•) at T_o = 298 K

a constant volume deformation process. For a constant volume uniaxial deformation the principal stretch ratio, $\lambda = l/l_o$, in the loding direction is related to the lateral sample dimension, r_i, by $r_i/r_o = x = x_o \lambda^{-1/2}$, where, l_o, l, are the initial and deformed sample lengths, and, x_o, x, are the dimensionless ratios of sample/cell radius in the initial and deformed state, respectively. Substituting, $x = x_o/\lambda^{-1/2}$, in Eq. (19)

$$G(\lambda) = G(0)\left[1 - \frac{5}{2}\left(\frac{T_o}{T_{ref}}\right)^2 \frac{x_o}{\sqrt{\lambda}} + \frac{14}{3}\left(\frac{T_o}{T_{ref}}\right)^2 \frac{x_o^2}{\lambda}\right] \quad (20)$$

Evaluating Eq. (20) at, $\lambda = 1$, and, $\lambda = 5$, for $T_o = T_{ref} = 298$ K; $x_o = 0.045$ ($r_i = 0.5$ mm), it is found that $G(\lambda = 5)/G(\lambda = 1) = 1.061$. An increase in $G(x)$ of about 6% is therefore associated with the lateral contraction of a 1 mm diameter sample going from the undeformed state to 400% strain ($\lambda = 5$) in the calorimeter at constant volume.

The relative importance of conductive and radiative heat transport on the pressure response of the calorimeter was determined by calculating $G(x)$ for a Nichrome wire heat source of zero emissivity, i.e., by setting, $\varepsilon = 0$, in Eq. (15). Figure 6 shows calculated results for $G(x)$ *vs.* heating wire diameter

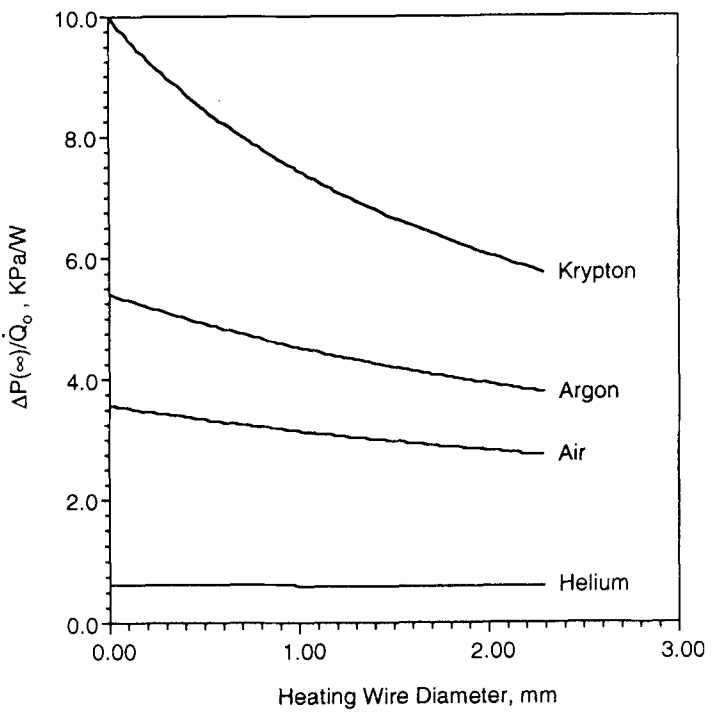

Fig. 7 Calculated steady-state pressure/heat flow ratio, $G(x)$, for gases; Krypton, Argon, Air and Helium in calorimeter

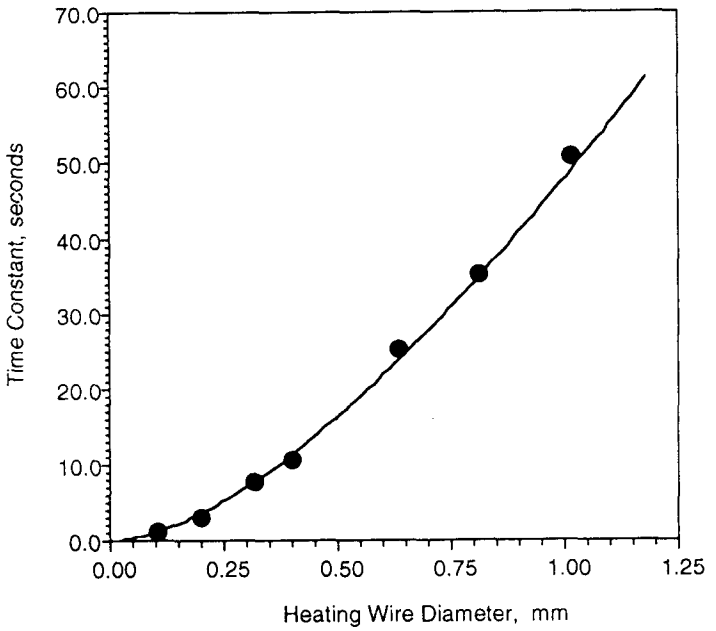

Fig. 8 Measured (•) and predicted (—) time constant *vs.* heating wire diameter

at 298 K for pure conduction (dashed line) compared to the combined conduction/radiation result (solid line) from Fig. 5. Also plotted in Fig. 6 are the measured $\Delta P(\infty)/Q_i^\circ$ values from Table 1. The predicted fall-off in $\Delta P(\infty)/Q_i^\circ$ with source diameter is a gas-thickness effect in the conduction case, with an added radiative surface area effect in the combined conduction/radiation case (Eq. (15)). The fraction of the total heat transported by radiation through the non-absorbing gas (air) increases from zero to about twenty-five percent with increasing source diameter over the range studied. Source size effects on steady-state gas pressure arise from the competition between radiant and conductive heat transfer as determined by the magnitude of the ratio, $\beta = 4r_i\varepsilon_i\sigma T_o^3/k_g$, in the denominator of the integrand of Eq. (15). It is clear the a combined conduction/radiation heat transfer mode must be invoked to capture the experimental data for steady-state gas pressure.

The effect of gas thermal conductivity on the steady-state pressure/heat flow ratio was calculated using Eq. (15) for gases; krypton (k_g= 0.0093 W/m-K), argon (k_g= 0.0172 W/m-K), air (k_g= 0.0261 W/m-K), and helium (k_g= 0.1482 W/m-K) at 298 K. Figure 7 shows the results of these calculations for $G(x)$ *vs.* source diameter. As the thermal conductivity of the gas increases calorimeter sensitivity decreases but source diameter effects become less pronounced.

Time constant τ values listed in Table 2 for the 15 cm long wires show a pronounced dependency on wire diameter (i.e., source dimensions) but only a minor dependence on cell temperature. The measured time constant at T_o= 298 K for each wire radius is plotted in Fig. 8 along with calculated values using Eq. (9) for heating wire properties, ρ= 8500 kg/m^3, C= 500 J/kg-K, and, ε= 1.0, along with the tabulated value, k_g= .0261 W/m-K, for the thermal conductivity of air at 298 K. It is observed that the agreement between measured and calculated time constants is very good for the range of source dimensions tested.

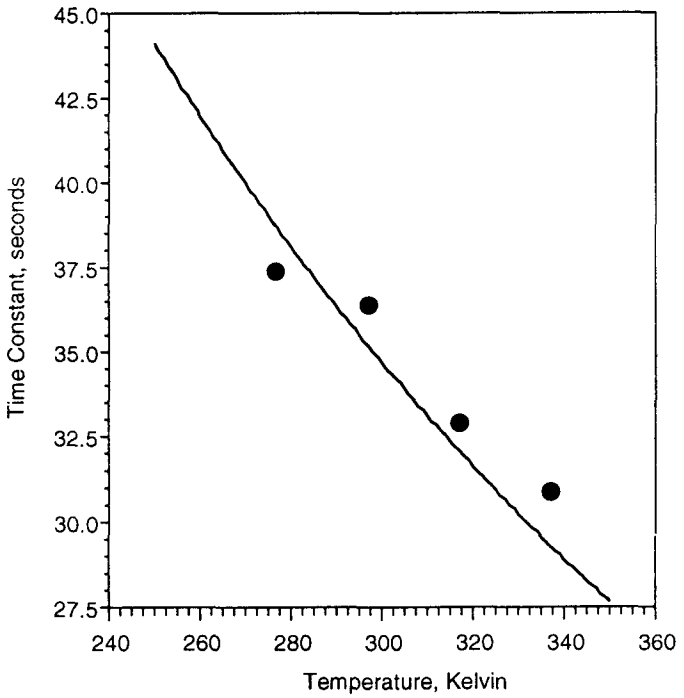

Fig. 9 Measured (•) and predicted (—) time constant *vs.* temperature for 0.813 mm diameter heat source in calorimeter

According to Eq. (9) the effect of temperature on τ is primarily through the temperature dependence of the gas thermal conductivity, and to a lesser extent, the radiant temperature of the source. Values for the thermal conductivity of the air in the calorimeter cell over the temperature range examined were determined by interpolation of tabulated values (6) using the expression $k_g(T)$= .0028+ 7.8×10^{-5} T(K). Figure 9 is a plot of measured and calculated time constants, τ, for the 15 cm long, 0.813 mm diameter heating wire *vs.* temperature. Agreement between measured and calculated values appears acceptable. Similar agreement was obtained for other wire diameters.

Conclusions

The transient and steady-state response of a gas-pressure deformation calorimeter are well represented by a simple, one-dimensional, linear, axisymmetric model of the calorimeter containing a lumped heat source. Conductive heat transport between the source and the cell wall is responsible for the observed gas-pressure change in the calorimeter at constant volume. Radiant heat transport through the non-absorbing gas produces no pressure change but can account for a significant fraction of the heat flow as the surface area of the source becomes appreciable. The transient pressure response is dominated by the relative size and thermal capacitance of the source and surrounding gas in the calorimeter in a predictable way. Agreement is generally good between experimental data and model predictions of calorimeter response over the range of source dimensions, heating rates, and test temperatures investigated in the study, providing useful insight into the advantages and limitations of this calorimetric technique.

* * *

The authors would like to acknowledge the partial support of this work by the U.S. Department of Energy and the Lawrence Livermore National Laboratory under Contract Number W-7405-ENG-48.

Definition of terms

A_i	Surface area of the heat source
A_o	Surface area of the calorimeter cell wall
β	Dimensionless ratio of radiant to conduction terms
C	Heat capacity of heat source
$\varepsilon_i, \varepsilon_o$	Emissivity of source and cell wall, respectively
$G(x)$	Derived geometric quantity relating gas pressure change to source and cell parameters
$G(0)$	Value of $G(x)$ at $x= 0$, i.e. line source
k_g	Thermal conductivity of gas in calorimeter
k_s	Thermal conductivity of heat source in the calorimeter
l_o, l	Sample length in the undeformed and deformed state, respectively
L	Calorimeter cell length= 0.287 m
λ	Principle stretch ratio of sample in loading direction, $\lambda= l/l_o$
P_o	Atmospheric pressure= 1 bar= 100 KPa
$\Delta P(t)$	Instantaneous gas pressure change in calorimeter resulting from heat flow
θ	Temperature difference between the source and calorimeter cell wall

$\dot{Q}_i^o$ Total heat flow from source (constant)
$\dot{Q}_i$ Total heat flow from source (variable)
$\dot{Q}_c$ Heat flow from source due to conduction
$\dot{Q}_r$ Radiant heat flow from source
r_i Source radius
r_o Calorimeter cell radius = 11.1 mm
ρ Density of heat source
σ Stefan-Boltzmann radiation constant
T_i Heat source temperature
T_o Calorimeter cell wall temperature
τ Time constant of source
V_i Volume of source
Ω Electrical resistance of heating wires
x Dimensionless ratio of source to cell radii
ξ Time variable of integration

References

1 R. E. Lyon and R. J. Farris, Rev. Sci. Inst., 57 (1986) 1640.
2 R. E. Lyon, Thermodynamics of Deformation, Ph. D. Thesis, University of Massachusetts, Amherst, MA, 1985.
3 R. E. Lyon and R. J. Farris, Polym. Eng. Sci., 24 (1984) 908.
4 J. P. Holman, Heat Transfer, McGraw-Hill 1963, Chapter 8.
5 R. E. Lyon and R. J. Farris, Thermochim. Acta, 161 (1990) 287.
6 D. R. Pitts and L. E. Sissom, Theory and Problems of Heat Transfer, McGraw-Hill Book Company, NY 1977, Appendix B.

Zusammenfassung — Ein einfaches eindimensionales axensymmetrisches Modell eines Gasdruck-Deformationskalorimeters erklärt die beobachteten Druckänderungen in Abhängigkeit der leitenden und strahlenden Komponenten des Wärmetransportes. Für die vorliegend untersuchten Bereiche von Strahlungsquellenabmessungen, Aufheizgeschwindigkeiten und Testtemperaturen wird im allgemeinen eine gute Übereinstimmung zwischen experimentellen Daten und vorausgesagter Kalorimeterwirkung beobachtet.